Immune Network
Immune Network

Characterization of Proinflammatory Responses and Innate Signaling Activation in Macrophages Infected with *Mycobacterium scrofulaceum*

Ki-Hye Kim[1], Tae-Sung Kim[3,4], Joy G. Lee[3,4], Jeong-Kyu Park[3,4], Miso Yang[3,4], Jin-Man Kim[4,5], Eun-Kyeong Jo[3,4]* and Jae-Min Yuk[2,4]*

[1]Center of Inflammation, Infection & Immunity, Institute for Biomedical Sciences, Georgia State University, Atlanta, GA, USA, Departments of [2]Infection Biology, [3]Microbiology, [4]Infection Signaling Network Research Center, [5]Department of Pathology, Chungnam National University School of Medicine, Daejeon 301-747, Korea

Mycobacterium scrofulaceum is an environmental and slow-growing atypical mycobacterium. Emerging evidence suggests that *M. scrofulaceum* infection is associated with cervical lymphadenitis in children and pulmonary or systemic infections in immunocompromised adults. However, the nature of host innate immune responses to *M. scrofulaceum* remains unclear. In this study, we examined the innate immune responses in murine bone marrow-derived macrophages (BMDMs) infected with different *M. scrofulaceum* strains including ATCC type strains and two clinically isolated strains (rough and smooth types). All three strains resulted in the production of proinflammatory cytokines in BMDMs mediated through toll-like receptor-2 and the adaptor MyD88. Activation of MAPKs (extracellular signal-regulated kinase 1/2, and p38, and c-Jun N-terminal kinase) and nuclear receptor (NF)-κB together with intracellular reactive oxygen species generation were required for the expression of proinflammatory cytokines in BMDMs. In addition, the rough morphotypes of *M. scrofulaceum* clinical strains induced higher levels of proinflammatory cytokines, MAPK and NF-κB activation, and ROS production than other strains. When mice were infected with different *M. scrofulaceum* strains, those infected with the rough strain showed the greatest hepatosplenomegaly, granulomatous lesions, and immune cell infiltration in the lungs. Notably, the bacterial load was higher in mice infected with rough colonies than in mice infected with ATCC or smooth strains. Collectively, these data indicate that rough *M. scrofulaceum* induces higher inflammatory responses and virulence than ATCC or smooth strains.

[Immune Network 2014;14(6):307-320]

INTRODUCTION

Mycobacterium scrofulaceum is a slow-growing environmental and opportunistic atypical mycobacterium that causes cervical lymphadenopathy in children and disseminated infection in adult patients with immunodeficiency (1). In addition, an extensively disseminated *M. scrofulaceum* infection was reported in an immunocompetent host with miliary lung lesions, lymphadenitis, granulomatous hepatitis, osteomyelitis, and subcutaneous abscesses (2). In Korea, *M. scrofulaceum* causes one of the most prevalent nontuberculous mycobacterial (NTM) pulmonary diseases, often found in immunocompetent patients (3). *M. scrofulaceum* is often classified as an MAIS organism (with *M. avium* and *M. intracellulare*). MAIS

*Corresponding Authors. Eun-Kyeong Jo and Jae-Min Yuk, Department of Infection Biology, and Infection Signaling Network Research Center, Chungnam National University School of Medicine, 6 Munhwa-dong, Jung-gu, Daejeon, Korea. Tel: 82-42-580-8272; Fax: 82-42-583-8216; E-mail: yjaemin0@cnu.ac.kr

Abbreviations: *M.scrofulaceum, Mycobacterium scrofulaceum*; NTM, nontuberculous mycobacterial; BMDMs, bone marrow-derived macrophages; PRR, pattern-recognition receptor; IKK, IκB kinase; CAPE, caffeic acid phenethyl ester

organisms are isolated from all parts of the environmental, especially drinking water and municipal water systems. Because MAIS organisms are generally resistant to most antimicrobial drugs, surgical excision often is used for treatment of lymphadenitis associated with atypical mycobacterial infection (4,5). However, the nature of the host immune response and pathogenic mechanisms that control the immune system in *M. scrofulaceum* infection remain unclear.

Growing evidence suggests that the innate immune system is an essential sentinel to protect the host as a primary and immediate defense during mycobacterial infection (6). Toll-like receptor is one of the most characteristic innate immune receptors and plays a crucial role in the initiation of inflammatory cytokine production and intracellular signaling to induce nuclear factor-κB activation in various cells infected with diverse mycobacterial strains (7-9). The activation of innate immune signaling induced by mycobacteria or their distinct components was shown to result in the production of proinflammatory cytokines and antimicrobial proteins in macrophages, promoting early control of mycobacterial infection (7,10). Triggering of innate immune receptors by mycobacterial ligands or mycobacteria leads to an activation of the mitogen-activated protein kinase (MAPK) pathway through TGF-β-activated kinase 1 (TAK1)-TAK1-binding protein (TAB) complex activation (11,12). In addition, the induction and activation of innate immune responses are crucial in shaping adaptive immune responses (13). In addition, mycobacterial infection triggers oxidative stress to increase the generation of intracellular reactive oxygen species, playing essential roles in signaling to mediate a variety of physiological functions in addition to pathogen killing in phagocytes (14,15). However, *M. scrofulaceum*-induced host innate immune responses and their regulatory mechanisms have not been fully elucidated, compared to those induced by *M. tuberculosis* or other NTM infection.

In this study, we examined not only the intracellular signaling pathways induced by *M. scrofulaceum* infection and underlying molecular mechanism, but also essential role of *M. scrofulaceum* morphotypes for regulating innate immune responses using ATCC type strains and clinically isolated two strains.

MATERIALS AND METHODS

Mice and cells

Wild-type 6-to-8-week-old female C57BL/6 mice were pur-chased form SAMTAKO BIO KOREA (Gyeonggi-do, Korea) and TLR2-, MyD88-, and TRIF-knockout (KO) mice on a C57BL/6 background were kindly provided by Dr. S. Akira (Osaka University, Japan). All animal procedures were approved by the Institutional Animal Care and Use Committee of Chungnam National University. Primary BMDMs were isolated from femurs of mice and then differentiated for 5~7 days in DMEM (Life Technologies BRL) containing macrophage colony stimulating factor (M-CSF, 25 ng/ml) (R&D systems, Minneapolis, MN, USA), 4 mM glutamine, and 10% FBS, as described previously (16).

Chemicals and reagents

All reagents and chemicals were purchased from Sigma-Aldrich except those noted below, which were obtained from the indicated suppliers. Specific Abs against phospho-ERK1/2 (Thr202/Tyr204), phospho-p38 (Thr180/Tyr182), and phospho-JNK (Thr183/Tyr185) were purchased from Cell signaling Technology (Cell signaling, Beverly, MA, USA). Specific inhibitors of MAPKs [U0126 (MEK inhibitor), SB203580 (p38 inhibitor), and SP600125 (JNK inhibitor)], the antioxidant *N*-acetyl-L-cysteine (NAC), diphenyleneiodonium (DPI) as an inhibitor of NADPH oxidase, BAY11-7082 (Bay), and caffeic acid phenethyl ester (CAPE) were purchased from Calbiochem (San Diego, CA, USA). Anti-β-actin (I-19) was purchased from Santa Cruz Biotechnology (Santa Cruz, CA, USA). Dimethyl sulfoxide (DMSO; Sigma-Aldrich, St. Louis, MO, USA) was added to cultures at a concentration of 0.1% (v/v) as a solvent control.

Bacterial strains, infection, and bacterial loads

M. scrofulaceum ATCC and clinical strains (KMRC 200-30113, -30114, -30115, -30116) were obtained from the Korean Institute of Tuberculosis (Osong, Chungbuk, Korea), maintained in Ogawa medium, and inoculated in Middlebrook 7H9 broth (Difco Laboratories, Detroit, MI, USA) supplemented with 10% oleic acid-albumin-dextrose-catalase (OADC) (BD Pharmingen, San Diego, CA, USA), 0.5% glycerol, and 0.05% Tween 80 (Sigma-Aldrich) at 37°C. Inocula were prepared from the mid-exponential-growth phase cultures. Bacteria were washed four times with cold PBS and then concentrated or diluted as needed. The number of colony-forming units (CFU) per milliliter was determined by plating on 7H10 agar supplemented with OADC at 37°C. For the *in vitro* experiments, macrophage infections were performed as described previously (16). Briefly, cells were infected with mycobacteria

at different MOIs and incubated for 4 h at 37°C in a 5% CO$_2$ atmosphere. After allowing time for phagocytosis, cells were washed four times with fresh PBS to remove extracellular bacteria and then incubated with complete DMEM without antibiotics. As controls, cultures of uninfected macrophages were maintained under the same conditions. For the *in vivo* experiments, a bacterial inoculum was prepared by thawing a frozen aliquot of a mycobacterium. Mice were intravenously injected with a suspension of 5×10^7 or 5×10^8 CFU bacteria per mouse in a final volume of 100 μl. Mice were euthanized at 0, 3, 7, 15, and 30 days after infection and the bacterial loads in the infected organs were determined by plating serial 10-fold dilutions of tissue homogenates on Middlebrook 7H10 medium supplemented with OADC. The plates were incubated for 4~6 weeks at 37°C. Control mice were injected with sterile saline.

Colony morphology and cord formation

Colony morphology was evaluated on 7H10 agar plates by microscopic observation. For detection of the cord formation, bacteria were cultured in 7H9 under stationary phase conditioned broth at 37°C for 7 days. Culture suspensions were spun onto glass slides using a cytocentrifuge and the bacteria were heat-fixed and then stained with crystal violet dye. Bacteria were examined at $\times$40 or $\times$100 magnification using a light microscope (Olympus, Japan) and photographed.

Quantitative and semi-quantitative RT-PCR

BMDMs or mice were infected as indicated in the figures and processed for analysis by RT-PCR, Western blot, and sandwich ELISA as described previously (16). Briefly, total RNA was isolated from BMDMs or lungs of mice using TRIzol reagent (Invitrogen, Carlsbad, CA) according to the manufacturer's instructions. Then, semi-quantitative reverse transcription polymerase chain reaction (RT-PCR) and real-time quantitative PCR were performed. The sequences of the primers used are as follows: TNF-α (forward) 5'-CGGACTCCGCAAAGTC-TAAG-3', (reverse) 5'-ACGGCATGGATCTCAAAGAC-3', IL-6 (forward) 5'-GGAAATTGGGGTAGGAAGGA-3', (reverse) 5'-CCGGAGAGGAGACTTCACAG-3', IL-12p40 (forward) 5'-GGA AGCACGGCAGCAGAATA-3', (reverse) 5'-AACTTGAGGGAG-AAGTAGGAATGG-3', β-actin (forward) 5'-TCATGAAGTGTG-ACGTTGACATCCGT-3', (reverse) 5'-CCTAGAAGCATTTGCG-GTGCACGATG-3'. PCR was performed as follows: For proinflammatory cytokine PCR, 30 cycles of denaturation at 95°C for 1 min, annealing at 58°C for 1 min, and extension at 72°C

for 1 min, with a final extension at 72°C for 10 min. Real-time PCR was performed using SYBR Green PCR Master Mix (Molecular Probes, Carlsbad, CA, USA), and transcript levels were quantified using an ABI 7900 Sequence Detection System (Applied Biosystems). The mean value of triplicate reactions was normalized against the mean value for β-actin.

NF-κB luciferase assay and immunofluorescence analysis of NF-κB p65 translocation

For the NF-κB luciferase assay, BMDMs were transduced with NF-κB p65 luciferase reporter adenovirus [20 plaque-forming units (PFU)/cell] constructs. After 36 h, the culture medium was changed to new medium and then cells were infected with MS strains (MOI=1, 5, 10). After 4 h, the cells were harvested in lysis buffer and luciferase activity was measured by a dual luciferase assay (Promega, Madison, WI, USA) as recommended by the manufacturer.

NF-κB p65 translocation was detected by immunofluorescence microscopy analysis as described previously (9). Briefly, BMDMs differentiated on coverslips were infected with MS strains at 37°C for 6 h, fixed with 4% (w/v) paraformaldehyde in PBS for 10 min at RT, permeabilized with 0.25% (v/v) Triton X-100 in PBS for 15 min at RT, and then blocked with 3% bovine serum albumin (BSA) in PBS for 1 h. Cells were immunostained with rabbit anti-mouse NF-κB p65 (1:400) for 2 h and the staining was detected using Alexa Fluor 488-conjugated anti-rabbit immunoglobulin (Ig) G (1:400, Molecular Probes, Eugene, OR, USA) for 1 h at RT. Nuclei were stained by incubation with 1 μg/ml 4',6'-diamidino-2-phenylindole (DAPI; Sigma-Aldrich). After mounting, fluorescence images were acquired with a confocal laser scanning microscope (DP ver. 1.2.108, Olympus).

Western blotting and enzyme-linked immunosorbent assay (ELISA)

For immunoblot analysis, primary Abs were diluted 1:1,000. Membranes were developed using a chemiluminescent reagent (ECL; Pharmacia-Amersham, Freiburg, Germany) (17). In sandwich ELISA, the levels of TNF-α, IL-6, and IL-12p40 in cell culture supernatants were analyzed using DuoSet antibody pairs (BD Pharmingen), according to the manufacturer's protocol.

Determination of cellular ROS

ROS production was measured by DHE assay, as previously described (8). Briefly, BMDMs were infected with MS strains

(MOI=5, 10) for 30 min and washed three times with phosphate-buffered saline (PBS) to remove extracellular bacteria. The cells were incubated with $2 \mu M$ DHE dye to detect superoxide for 30 min at $37^{\circ}C$ in 5% CO_2 and then fixed with 4% paraformaldehyde in PBS at room temperature (RT) followed by flow cytometry using a FACSCanto II flow cytometer (Becton Dickinson, San Jose, CA, USA) and FlowJo software (Tree Star, Ashland, OR, USA).

Pulmonarly histopathology and immunohistochemical staining

Mice were sacrificed at 0, 3, 7, 15, and 30 days after infection with MS strains and lung tissue was collected from individual mice. Lung tissues were fixed in 10% formalin and then dehydrated, paraffin-embedded, and sectioned at $5 \mu m$. Sections of lung tissues were stained with haematoxylin and eosin for histopathological analysis. Morphometric image analysis was performed at ×100 or ×200 magnification. For immunohistochemical staining of COX-2, paraffin-embedded lung sections were stained using rabbit anti-mouse polyclonal COX-2 antibody (Abcam, Cambridge, UK), biotin-conjugated rabbit anti-mouse IgG, and a peroxidase-conjugated streptavidin antibody. Then, visualization was performed with 3,3-diaminobenzidine as the peroxidase substrate (Sigma-Aldrich).

Statistical analysis

The data were obtained as the mean ($\pm$standard deviation) value from independent experiments on 3~5 mice per group. The statistical analyses were performed using Student's *t*-test with Bonferroni correction or analysis of variance in addition to two-way ANOVA using GraphPad Prism version 5 (GraphPad software Inc, San Diego, CA, USA). $p < 0.05$ was considered significant.

RESULTS

M. scrofulaceum 114R strain induces enhanced proinflammatory cytokine responses compared to other strains

Previous studies demonstrated that the morphotype of mycobacteria is associated with virulence (18,19). To identify the correlation between morphotype and host immune responses of *M. scrofulaceum*, we prepared various strains of *M. scrofulaceum* including ATCC 19991 (ATCC), clinically isolated KMRC 00200-30113 (113S), MS KMRC 00200-30114 (114R), KMRC 00200-30115 (115S), and KMRC 00200-30116 (116S).

Microscopic images indicated that only colonies of the 114R strain had a rough morphology similar to that of the *M. tuberculosis* virulent strain (H37RV) (Fig. 1A). We next examined whether the colony morphology affects the production of proinflammatory cytokines such as tumor necrosis factor (TNF)-α, interleukin (IL)-6, and IL-12p40. We infected bone marrow-derived macrophages (BMDMs) with the ATCC, 113S, or 114R strains of *M. scrofulaceum* and examined the mRNA and protein expression of proinflammatory cytokines. As shown in Fig. 1B, the cells infected with 114R showed higher mRNA expression of TNF, IL-6, and IL-12p40 than those infected with ATCC or 113S at both 3 h and 6 h of infection. Consistent with these findings, protein expression of proinflammatory cytokines was highly increased in cells infected with 114R compared with those infected with ATCC, 113S, 115S, 116S in concentration- and time-dependent manners (Fig. 1C). These findings indicate that *M. scrofulaceum*-mediated proinflammatory responses depend on colony morphotype.

The TLR2/MyD88 pathway, but not TRIF, is required for production of proinflammatory cytokines in *M. scrofulaceum*-infected macrophages

Numerous studies have reported that mycobacteria and their antigenic components activate intracellular signaling cascade through innate recognition of TLRs (9,12,16,17,20). To determine the roles of TLR2 in mycobacteria-induced production of proinflammatory cytokines in macrophages, BMDMs from TLR2 wild type (WT) and knockout (KO) mice were stimulated with ATCC, 113S, or 114R strains of *M. scrofulaceum* in an MOI-dependent manner. As shown in Fig. 2A, the mycobacteria-induced production of TNF, IL-6, and IL-12p40 was absolutely inhibited in BMDMs from TLR2 KO mice. Because the adaptor proteins MyD88 and TRIF are essential for signal transduction of TLR (21), we further examined whether the production of these three strain-induced cytokines was dependent on either MyD88 or TRIF. BMDMs from MyD88 KO mice but not from TRIF KO mice showed a significant decrease of TNF, IL-6, and IL-12p40 levels after infection with each of the strains (Fig. 2B). These results suggest that the TLR2/MyD88 signaling pathway is important for host inflammatory responses in *M. scrofulaceum* infection.
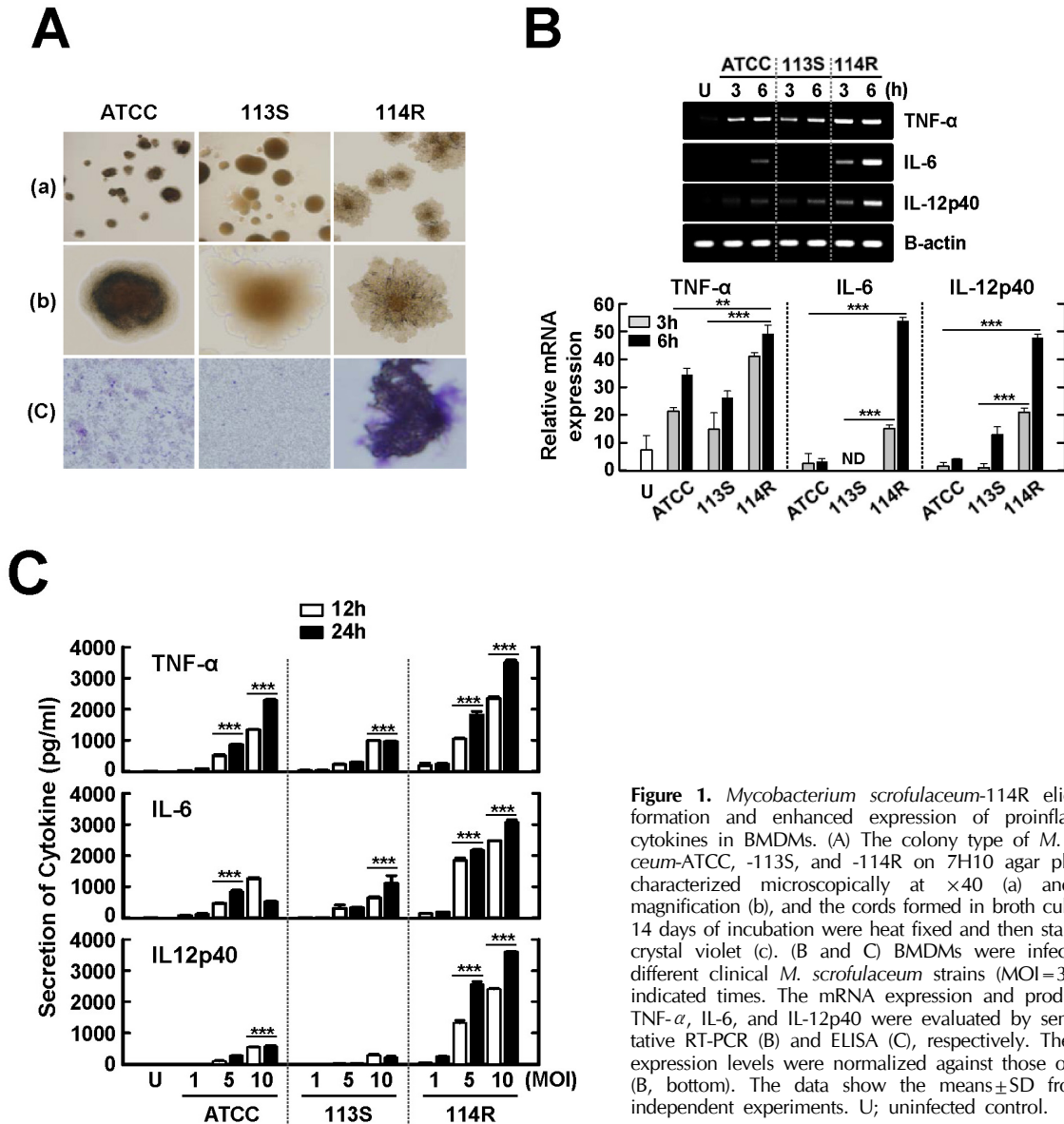
Figure 1. *Mycobacterium scrofulaceum*-114R elicits cord formation and enhanced expression of proinflammatory cytokines in BMDMs. (A) The colony type of *M. scrofulaceum*-ATCC, -113S, and -114R on 7H10 agar plates was characterized microscopically at ×40 (a) and ×100 magnification (b), and the cords formed in broth culture after 14 days of incubation were heat fixed and then stained with crystal violet (c). (B and C) BMDMs were infected with different clinical *M. scrofulaceum* strains (MOI = 3) for the indicated times. The mRNA expression and production of TNF-α, IL-6, and IL-12p40 were evaluated by semi-quantitative RT-PCR (B) and ELISA (C), respectively. The relative expression levels were normalized against those of β-actin (B, bottom). The data show the means ± SD from three independent experiments. U; uninfected control.

NF-κB signaling is critical for enhanced proinflammatory responses against infection by *M. scrofulaceum* 114R

As a consequence of cross-talk between pattern-recognition receptors (PRRs) and mycobacteria, inflammatory responses are mainly initiated by a conserved signaling pathway involving NF-κB activation (12). We therefore examined NF-κB luciferase activity and nuclear translocation in BMDMs infected with the ATCC, 113S, or 114R strains of *M. scrofulaceum*. As shown in Fig. 3A, 114R-infected cells showed higher NF-κB luciferase activity than cells infected with ATCC or 113S in a dose-dependent manner. NF-κB nuclear translocation is followed by phosphorylation of the IκB kinase (IKK) complex and the inhibitor of NF-κB proteins (IκB)-α, which is critical for the transcriptional activation of target genes including proinflammatory cytokines (22). We found that 114R infection resulted in a greater enhancement of nuclear translocation of p65 (Fig. 3B) than ATCC or 113S infection. In addition, pre-
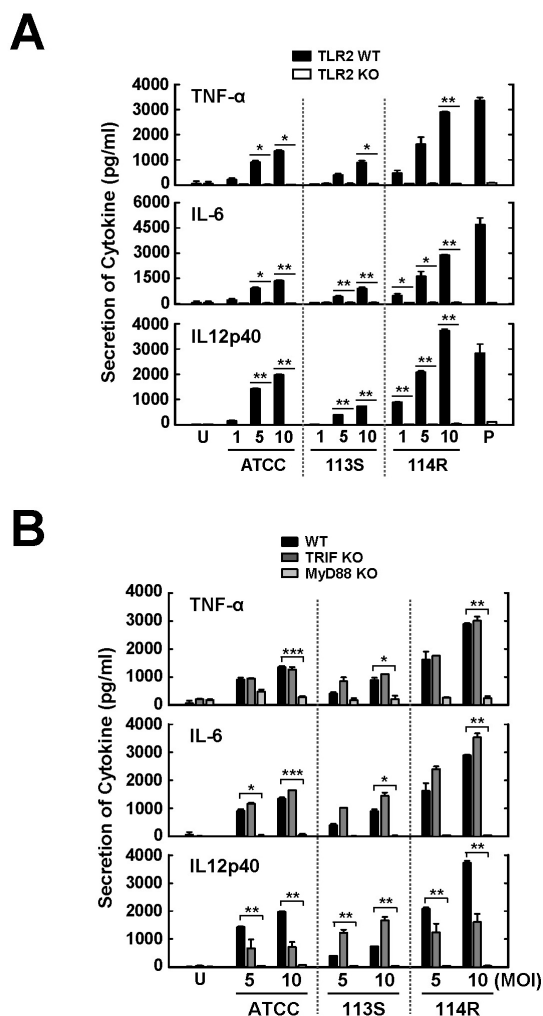
Figure 2. *Mycobacterium scrofulaceum*-induced proinflammatory cytokine production is mediated by TLR2/MyD88 signaling. (A and B) BMDMs isolated from WT and TLR2 KO mice (for A) or WT, MyD88, and TRIF KO mice (for B) were stimulated with *M. scrofulaceum*-ATCC, -113S, and -114R (MOI = 1, 5, 10) for 18 h. The levels of TNF-α, IL-6, and IL-12p40 in the supernatants were measured by ELISA. Pam$_3$CSK$_4$ (P; 100 ng/ml) was used as positive ligand for TLR2. The data represent the mean±SD from three independent experiments. U; uninfected control.

Figure 3. *Mycobacterium scrofulaceum*-114R strongly increases the production of proinflammatory cytokines through NF-κB signaling in BMDMs. (A) BMDMs were transduced with NF-κB p65 adenovirus luciferase construct (20 PFU/cells) for 36 h and then infected with *M. scrofulaceum*-ATCC, -113S, -114R (MOI = 1, 5, 10) for 4 h. Cell lysates were harvested and luciferase activity was measured. (B) BMDMs were infected with M. scrofulaceum strains (MOI = 5) for 30 min and then immunolabeled with anti-NF-κB p65 antibody and anti-rabbit-AlexaFluor 488 (green), and the nuclei were stained with DAPI (blue). Representative immunofluorescence images (left panel) and the average mean fluorescence intensity of cells exhibiting NF-κB nuclear translocation (right panel) are shown. (C) BMDMs were preincubated in the presence or absence of BAY11-7082 (BAY; 0.3, 1, 3 μM) or CAPE (1, 5, 10 μM) for 45 min prior to infection with *M. scrofulaceum* strains (MOI = 5). The mRNA expression and production of TNF-α and IL-6 were evaluated by semi-quantitative RT-PCR. The data show the mean±SD from three independent experiments. U; uninfected control, SC; solvent control (0.1% DMSO).

treatment with NF-κB specific inhibitors including Bay 11-7085 (BAY) and caffeic acid phenethyl ester (CAPE) significantly inhibited the mRNA expression of 114R-induced proinflammatory cytokines such as TNF-α and IL-6 (Fig. 3C). These results suggest that 114R activated NF-κB signaling more strongly than ATCC or 113S to produce proinflammatory cytokines.
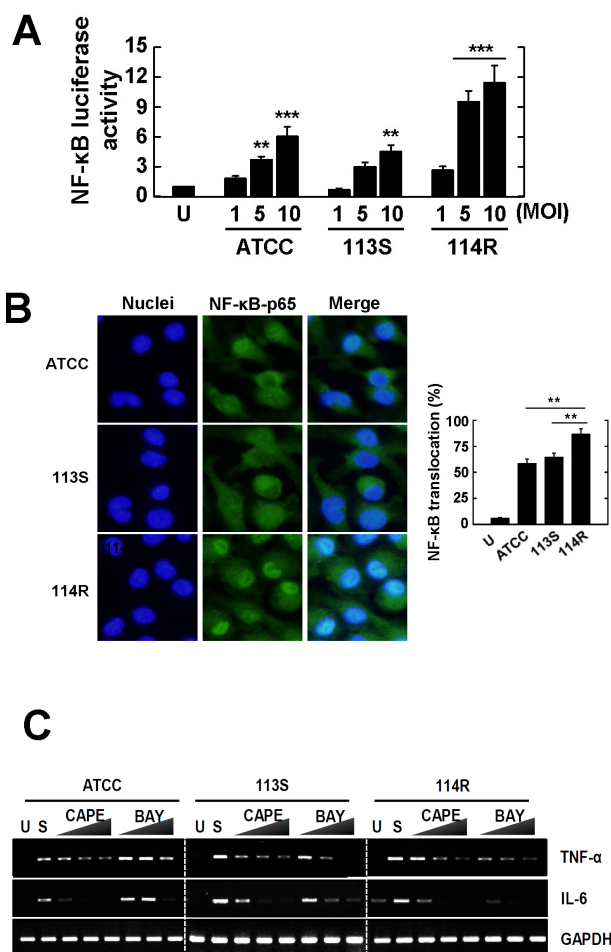
M. scrofulaceum 114R strain actively induces MAPK activation in macrophages

We previously found that mycobacterial infection induced
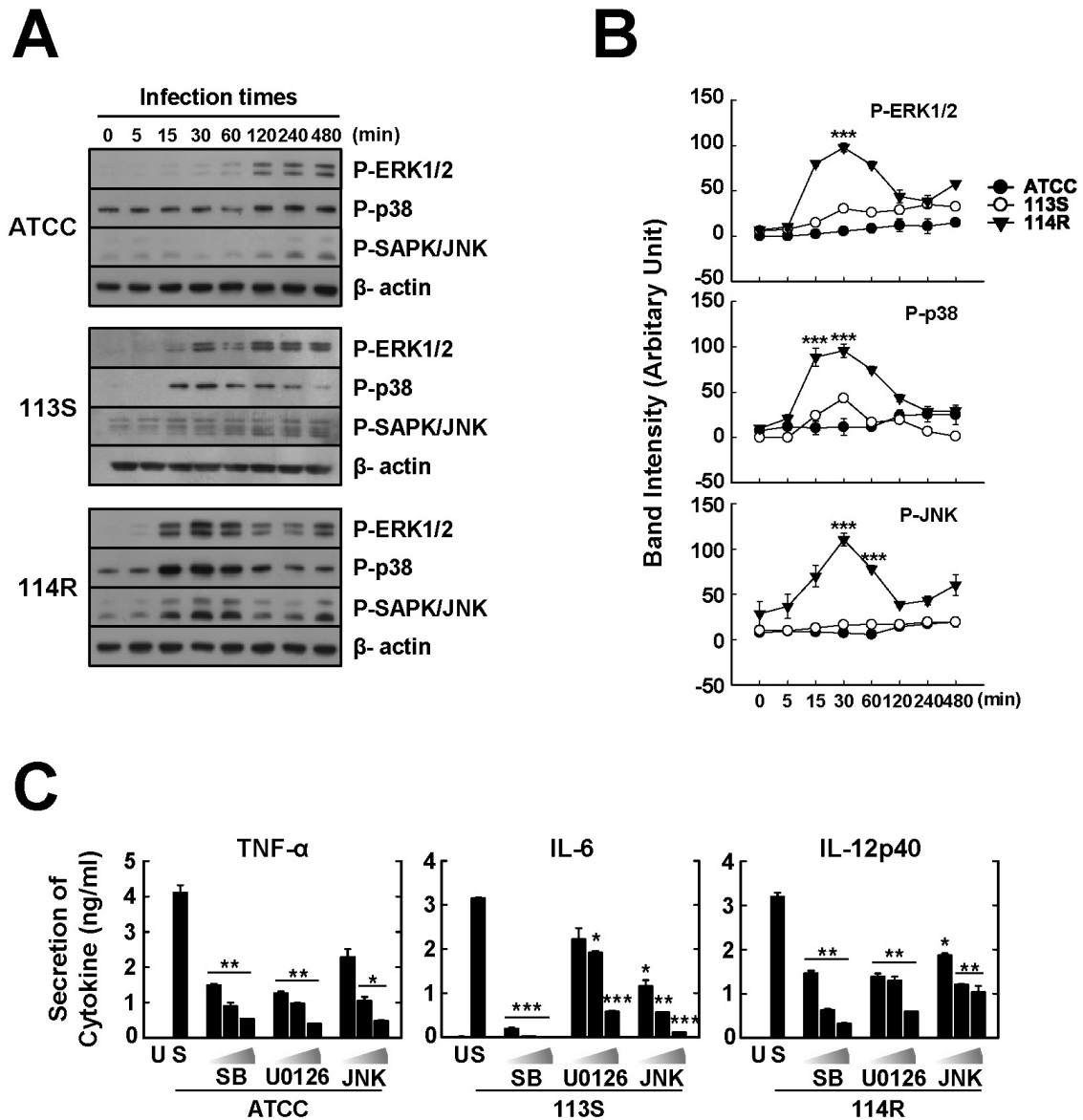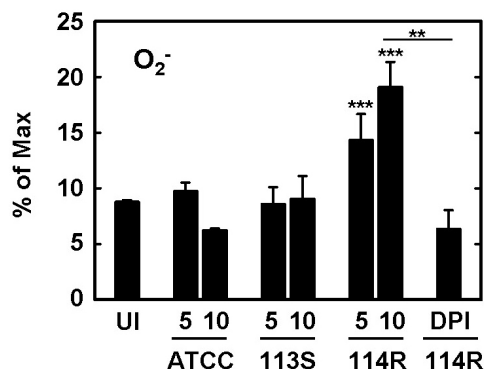
Figure 4. *Mycobacterium scrofulaceum* 114R-induced pro-inflammatory cytokine production is modulated through MAPK signaling in BMDMs. (A) Kinetics of phospho- RK1/2, -p38, and -SAPK/JNK in BMDMs infected with *M. scrofulaceum*-ATCC, -113S, and -114R (MOI=5). The cell lysates were collected at the indicated times and phosphorylated MAPKs were examined by western blot analysis. β-ctin was used as a loading control. (B) Expression levels were normalized against those of β-actin (C) BMDMs were pretreated with p38 inhibitor (SB203580; 1, 5, and 10 μM), MEK-1 inhibitor (U0126; 5, 10, and 20 μM), and JNK inhibitor (JNK; 5, 10, and 20 μM) for 45 min prior to infection with different *M. scrofulaceum* strains (MOI=5). The culture supernatants were harvested at 18 h, and the production of TNF-α, IL-6, and IL-12p40 cytokines was measured by ELISA. The data show the mean$\pm$SD of three independent experiments. Significant differences: [#]$p<0.05$ compared with uninfected control; *$p<0.05$, **$p<0.01$, and ***$p<0.001$ compared with solvent control. U; uninfected control, SC; solvent control (0.1% DMSO).

phosphorylation of MAPK such as p38, JNK, and ERK1/2, resulting in production of inflammatory cytokines (16,20). To determine whether *M. scrofulaceum*-induced inflammatory re-

sponses were dependent on MAPK signaling, we monitored MAPK activation in macrophages. Although these three strains induced phosphorylation of p38, SAPK/JNK and ERK1/2, the
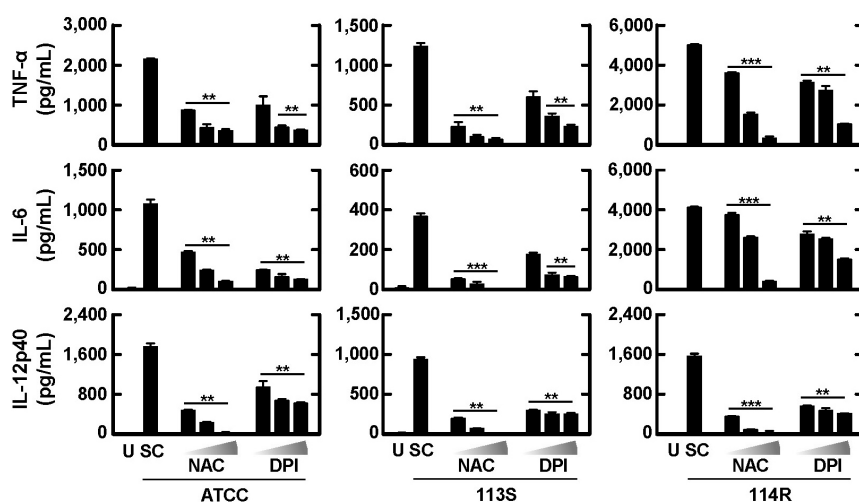
A

B

Figure 5. ROS signaling-mediated proinflammatory cytokine production in *Mycobacterium scrofulaceum*-infected BMDMs (A) BMDMs were infected with *M. scrofulaceum*-ATCC, -113S, or -114R (MOI 5, 10) for 30 min and then stained with DHE for 30 min. Superoxide-roducing cells were analyzed by flow cytometry. (B) BMDMs were incubated with NAC (10, 20, and 30 mM) or DPI (1, 5, and 10 μM) before infection with different *M. scrofulaceum* strains (MOI = 5). The supernatant was harvested at 20 h, and cytokine production was measured by ELISA. The data show the mean $\pm$ SD of three independent experiments. Significant differences: **p $<$ 0.01 and ***p $<$ 0.001 compared with solvent control. U; uninfected control, SC; solvent control (0.1% DMSO).

114R strain especially induced rapid and strong activation within 30 min (Fig. 4A and B). We next investigated the role of MAPK signaling in proinflammatory cytokine production induced by the 114R strain. As shown in Fig. 4C, pretreatment with specific inhibitors of JNK (SP600125), p38 (SB203580), or MEK (U0126) caused significant inhibition of 114R-induced TNF-α, IL-6, and IL-12p40 production in a concentration-dependent manner (Fig. 4C). Together, these results suggest that the 114R strain strongly induces the production of proinflammatory cytokines through enhanced activation of MAPK signaling compared to ATCC or 113S in macrophages.

NADPH oxidase-dependent ROS generation regulates inflammatory responses to *M. scrofulaceum* infection in macrophages

Previous studies proposed that Gp91phox/NADPH oxidase (NOX) 2 is critical for regulation of TLR-mediated inflammatory responses and host innate immune responses against *M. tuberculosis* (15) and *M. massiliense* (20). We first investigated whether *M. scrofulaceum* induced intracellular superoxide production in BMDMs using the oxidative fluorescent dye dihydroethidium (DHE). Flow cytometric analysis (Fig. 5A) showed that 114R infection, but not that of ATCC or 113S, strongly induced superoxide generation at MOI 5 and 10. We further examined whether 114R-induced ROS gen-
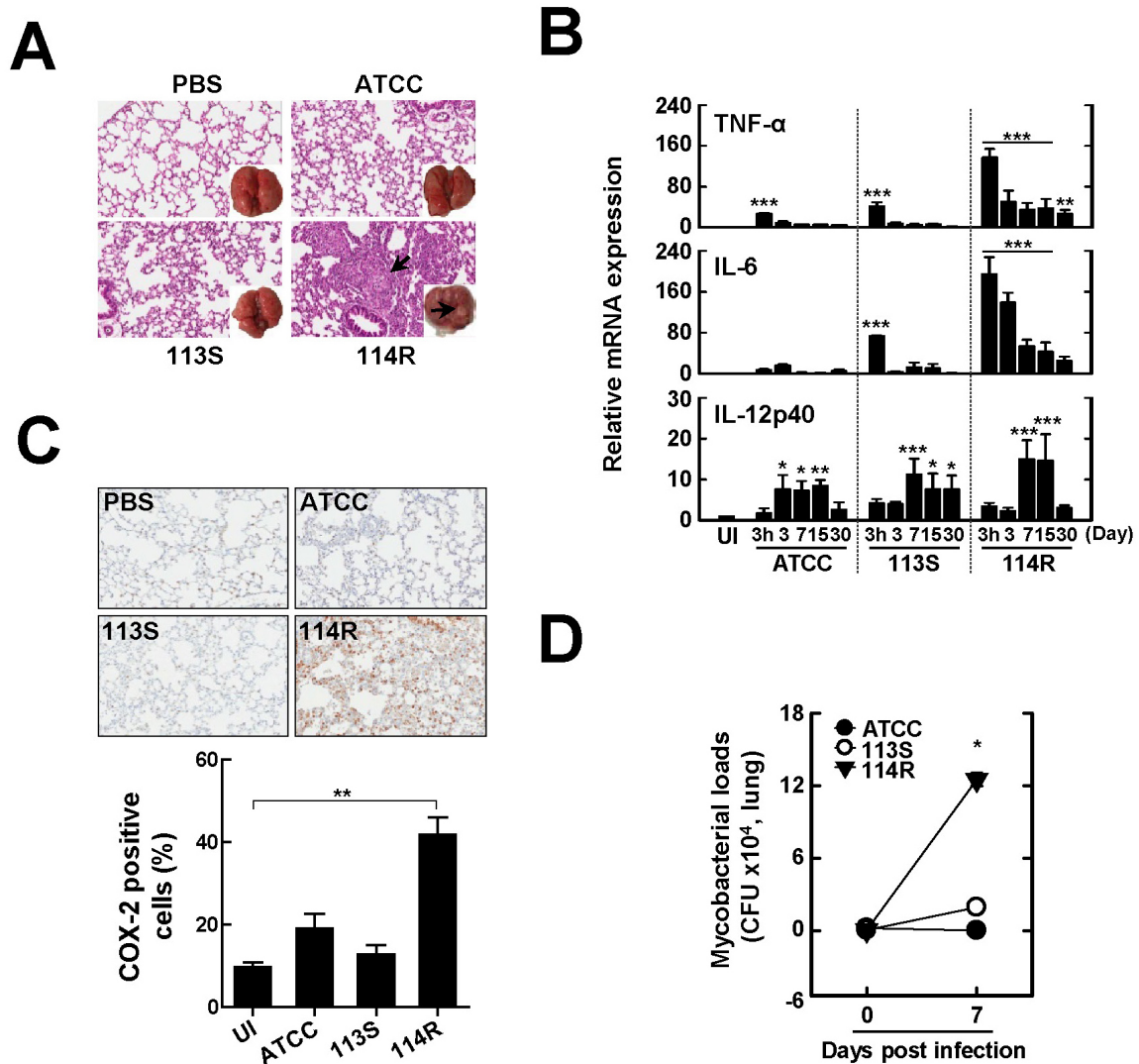
Figure 6. *Mycobacterium scrofulaceum*-114R infection induces granulomatous lesion formation, higher mycobacteria burden and inflammation in the lung C57BL/6 mice were infected intravenously with 5×10^7 CFU of *M. scrofulaceum*-ATCC, -113S, or 114R or treated with saline (UI) for the indicated periods of time. (A) Lung tissues were collected and fixed with 10% formalin and paraffin-embedded. Lung sections were stained with hematoxylin and eosin (H&E). Inflammatory cell infiltration, granulomatous lesions, and lung histology were observed at ×100 (upper) or ×200 (bottom) magnification; the black arrowhead in the panel indicates the granulomatous lesion. (B) mRNA expression of TNF-α, IL-6, and IL-12p40 cytokines in the lungs was determined by real-time PCR analysis. (C) Expression of COX-2 in lungs of mice infected with *M. scrofulaceum* strains was examined at 14 days post-infection by immunohistochemical staining of COX-2. (D) The mycobacterial loads of the lungs were determined at 0 and 7 days post-infection. The data show the mean±SD of three individual mice per group. Significant difference: *p<0.05, compared to *M. scrofulaceum*-ATCC or -113S-infected mice; **p<0.01 compared with the uninfected control (UI).

eration was essential for the production of proinflammatory cytokines in macrophages infected with the three strains. As shown in Fig. 5B, pretreatment with the general ROS scavenger NAC and NADPH oxidase inhibitor DPI significantly attenuated the production of TNF-α in a concentration-dependent manner. These data suggest that 114R activated ROS gen-

eration more strongly than ATCC or 113S, which resulted in hyperactivation of inflammatory responses.

Lungs of mice infected with different M. scrofulaceum stains exhibit histological changes and bacterial loads with the progression of infection

Mycobacterial infection is known as a major source of granulomatous reactions in humans and in animal models (23). We first investigated whether infection by *M. scrofulaceum* ATCC, 113S, and 114R strains induced granuloma formation in a murine model. At day 7, 114R-infected mice showed a stronger granulomatous response and infiltration of immune cells (Fig. 6A) than ATCC- or 113S-infected mice. In comparison to animals infected with the ATCC or 113S strain, 114R-infected mice showed significantly higher bacterial loads at day 7 post infection (Fig. 6D).

During *M. tuberculosis* infection, inflammatory responses are closely associated with granulomatous reactions (24). We thus examined the inflammatory responses in mice infected with the three strains. As shown in Fig. 6C, expression of cyclooxygenase-2, a key enzyme for activation of the inflammatory cascade, was significantly higher in the lungs of 114R-infected mice than in those of ATCC- or 113S-infected mice. We further analyzed the mRNA expression of proinflammatory cytokines in mouse lungs infected with the three strains. mRNA expression of TNF-α, IL-6, and IL-12p40 was higher in the lungs of 114R-infected mice than in those of ATCC or 113S-infected mice (Fig. 6B). Together, these data indicate that 114R infection induces strong inflammatory responses that finally result in enhanced granulomatous reactions.

DISCUSSION

M. scrofulaceum belonging to the MAIS organisms (with *M. avium* and *M. intracellulare*) (4) is associated with non-tuberculous mycobacterial (NTM) lymphadenitis and pulmonary disseminated infection in adult patients with or without immunodeficiency (1-3,25-27). *M. scrofulaceum* is an environmental mycobacteria isolated from soil and water in tropical regions (28) and also found in cooling towers that are suitable environments for potentially pathogenic mycobacteria (29).

M. scrofulaceum infection is relatively rare compared to infection by other MAIS organisms but appears to have clinical relevance associated with HIV infection in humans (1,30). In animal infection models, prior *M. scrofulaceum* infection (with two other mycobacterial strains, such as *M. avium* and *M. vaccae*) led to significant inhibition of BCG multiplication and reduced vaccination effects in sensitized mice (31). Thus, it is considered that priming immune host responses with environmental mycobacteria could reduce the protective effects of BCG infection or vaccination to a level insufficient to control *M. tuberculosis* infection (31,32). Despite these findings, the inducing activities and regulatory mechanisms of the slow-growing NTM *M. scrofulaceum* with respect to the host innate and inflammatory immune responses have been poorly characterized, compared to those of *M. tuberculosis* or rapidly growing NTMs. In the present study, we found that R isolates formed multicellular cords, similar to those observed in *M. tuberculosis*, but S isolates did not. We then subjected each morphotype to further immune studies. We found that *M. scrofulaceum*-infected macrophages showed a robust induction of proinflammatory cytokine expression, and the R morphotype of *M. scrofulaceum* clinical isolates induced higher cytokine production than type strains and the S morphotype.

Although previous studies described the R morphology of a *M. avium-M. intracellulare-M. scrofulaceum* complex lacking outer cell wall C-mycoside glycopeptidolipids (GPLs) (33), the present data on increased induction of inflammatory responses by the *M. scrofulaceum* R morphotype partially supports the findings of previous studies in other NTM strains showing the induction of enhanced immune and inflammatory responses by R type NTM strains. In certain NTM strains, the S morphotypes usually contain GPLs that are found in the outermost part of the cell envelope and also play a key role in biofilm formation (18,34). The R type that lacks GPLs can multiply in host macrophages and cause persistent infection although it cannot form biofilms (18). Recently, it was shown that the massive production of serpentine cords by the R variant of *M. abscessus* contributes to resistance against phagocytosis in macrophages or neutrophils and induces abscess formation and increased virulence in zebrafish models (35). In addition, the R type of *M. abscessus* activates innate immune responses in macrophages through TLR2, suggesting that GPLs on NTM cell walls mask the underlying mycobacterial lipids, thereby promoting innate immune responses and airway inflammation (36). Recent studies also showed that human monocytes were not able to internalize the R type of *M. abscessus* and induced higher IL-1β production and lower IL-10 production than the S type (37). Taken together, the current observations that the R type of *M. scrofulaceum* induced increased proinflammatory responses in macrophages are consistent with previous findings for other NTM strains, especially *M. abscessus*.

TLR2 and MyD88 are required for early proinflammatory cytokine generation in the macrophage response against *M. scrofulaceum* infection. Our data indicate a dependence on NF-κB to also drive inflammatory responses against *M. scrofulaceum*. Previous studies by us and others showed that TLR2-dependent signaling is important for NF-κB signaling and proinflammatory cytokine generation in macrophages in response to diverse mycobacterial strains including *M. tuberculosis*, *M. avium*, *M. abscessus*, and *M. massilience* (7-9,20,38,39). In addition, mycobacterial components, including lipomannans from *M. chelonae* and *M. kansasii* were shown to induce proinflammatory cytokine generation through TLR2 (40). *M. tuberculosis* was shown to recognize TLR2, TLR4, and TLR9 in initiating innate immune responses (38,41). The TLR adaptor MyD88 plays a key role in the activation of innate immune responses to mycobacterial infection. Based on these findings, MyD88-deficient mice have increased susceptibility for acute *M. tuberculosis* infection (42). In addition, MyD88-deficient macrophages and dendritic cells showed defective cytokine and nitric oxide production in response to mycobacterial infection (42). The current data demonstrate that TLR2-MyD88-NF-κB signaling is mainly required for *M. scrofulaceum*-induced innate immune responses in macrophages. TLR2-induced host immune responses are essential for the suppression of mycobacterial proliferation within macrophages but also function in mycobacterial escape through decreased MHC-II expression or antigen-processing ability (43).

The MAPK signaling pathway has been described to be involved in the generation of proinflammatory cytokines such as TNF-α, IL-6, and IL-12p40 during mycobacterial infection (7,44). TLR-induced MAPK signaling is required for the initiation of effective innate immune responses against mycobacterial components and *M. tuberculosis* (7,44,45). Our previous studies showed that MAPK activation in response to the mycobacterial 38-kDa antigen was highly increased in human monocytes from active pulmonary tuberculosis patients (46). Recently, it was shown that MAPK activation and pro- and anti-inflammatory cytokine secretion were significantly depressed in monocytes from patients with *M. abscessus* pulmonary diseases (47). Therefore, the analysis of the activation of the MAPK signaling pathway may contribute to an explanation of *M. tuberculosis* host susceptibility and atypical mycobacterial infection.

Phagocytized bacterial infection by host innate immune cells including mycobacteria initiates an oxidative burst re-

action (48). Generation of free radicals derived from phagocytes infected with human pathogens contributes to both effective defense and immune escape during microbial infection (49,50). Moreover, intracellular ROS are critical signaling mediators in immune cells for various physiological functions including TLR signaling in response to various types of microbial ligand stimulation (15). Our support previous findings that ROS signaling is required for inflammatory cytokine generation in macrophages infected with *M. massiliense* (20). Previous studies found that ROS generation is required for the ER stress-induced apoptosis in macrophages infected with clinical isolates of *M. kansasii* (51). Our earlier studies also showed that antimicrobial activity during anti-mycobacterial chemotherapy is dependent on cellular and mitochondrial ROS-mediated autophagy activation (52). In addition, oxidative stress induced by vitamin C has been found to be crucial for bactericidal activity against *M. tuberculosis* (53). Indeed, different *M. tuberculosis* strains have been shown to exhibit diverse patterns of ROS production (54). Because multidrug-resistant strains lack the ability to induce neutrophil apoptosis and ROS generation (54), it is tempting to speculate that the different ability to induce ROS generation among clinical strains is associated with disease pathology or human susceptibility to atypical mycobacterial infection.

Our *in vivo* data showed that the R morphotype of *M. scrofulaceum* induced increased pathology, granulomatous lesions, and immune cell infiltration in lungs, compared to the S morphotype or ATCC strain. In addition, the bacterial loads were higher in mice infected with the R morphotype than in those infected with other strains. Among different *M. avium* complex strains, smooth transparent variants, the most frequent types found in AIDS patients, showed increased virulency and mycobacterial multiplication in the lungs, livers, and spleens of mice than strains of other morphotypes (55). Furthermore, mouse studies using different strains of *M. abscessus* showed that differences among strains were highly associated with differences in virulence and distinct types of clinical disease including the upper lobe fibrocavitary form and nodular bronchiectatic form (56). Future studies should clarify whether the differences in pathology and virulence among diverse clinical strains is associated with the human host susceptibility to *M. scrofulaceum*. Together, our data indicate that *M. scrofulaceum* activates innate immune responses through the TLR2-MyD88-NF-κB, MAPK, and ROS signaling pathways. Among different strains, the R morphotype showed the greatest induction of inflammatory responses

and intracellular signaling activation. We further showed that the *in vitro* immune profile was highly correlated with the *in vivo* manifestation of infection by different strains. Characterization of immune signaling features may contribute to understanding the host-pathogen interaction for the development of novel therapeutics or preventives against *M. scrofulaceum* infection.

ACKNOWLEDGEMENTS

CONFLICTS OF INTEREST

The authors have no financial conflict of interest.

REFERENCES

1. Sanders, J. W., A. D. Walsh, R. L. Snider, and E. E. Sahn. 1995. Disseminated *Mycobacterium scrofulaceum* infection: a potentially treatable complication of AIDS. *Clin. Infect. Dis.* 20: 549.
2. Hsueh, P. R., T. R. Hsiue, J. J. Jarn, S. W. Ho, and W. C. Hsieh. 1996. Disseminated infection due to *Mycobacterium scrofulaceum* in an immunocompetent host. *Clin. Infect. Dis.* 22: 159-161.
3. Ryoo, S. W., S. Shin, M. S. Shim, Y. S. Park, W. J. Lew, S. N. Park, Y. K. Park, and S. Kang. 2008. Spread of non-tuberculous mycobacteria from 1993 to 2006 in Koreans. *J. Clin. Lab Anal.* 22: 415-420.
4. Falkinham, J. O., III. 2003. Factors influencing the chlorine susceptibility of *Mycobacterium avium*, *Mycobacterium intracellulare*, and *Mycobacterium scrofulaceum*. *Appl. Environ. Microbiol.* 69: 5685-5689.
5. Rosenzweig, D.Y. 1980. "Atypical" mycobacterioses. *Clin. Chest Med.* 1: 273-284.
6. Verrall, A. J., M. G. Netea, B. Alisjahbana, P. C. Hill, and C. R. van. 2014. Early clearance of *Mycobacterium tuberculosis*: a new frontier in prevention. *Immunology* 141: 506-513.
7. Jo, E. K., C. S. Yang, C. H. Choi, and C. V. Harding. 2007. Intracellular signalling cascades regulating innate immune responses to Mycobacteria: branching out from Toll-like receptors. *Cell Microbiol.* 9: 1087-1098.
8. Shin, D. M., C. S. Yang, J. M. Yuk, J. Y. Lee, K. H. Kim, S. J. Shin, K. Takahara, S. J. Lee, and E. K. Jo. 2008. *Mycobacterium abscessus* activates the macrophage innate immune response via a physical and functional interaction between TLR2 and dectin-1. *Cell Microbiol.* 10: 1608-1621.
9. Lee, H. M., D. M. Shin, D. K. Choi, Z. W. Lee, K. H. Kim, J. M. Yuk, C. D. Kim, J. H. Lee, and E. K. Jo. 2009. Innate immune responses to *Mycobacterium ulcerans* via toll-like receptors and dectin-1 in human keratinocytes. *Cell Microbiol.* 11: 678-692.
10. Torrado, E., and A. M. Cooper. 2013. Cytokines in the balance of protection and pathology during mycobacterial infections. *Adv. Exp. Med. Biol.* 783: 121-140.
11. Kawai, T., and S. Akira. 2006. TLR signaling. *Cell Death. Differ.* 13: 816-825.
12. Basu, J., D. M. Shin, and E. K. Jo. 2012. Mycobacterial signaling through toll-like receptors. *Front Cell Infect. Microbiol.* 2: 145.
13. Quigley, M., J. Martinez, X. Huang, and Y. Yang. 2009. A critical role for direct TLR2-MyD88 signaling in CD8 T-cell clonal expansion and memory formation following vaccinia viral infection. *Blood* 113: 2256-2264.
14. Schieber, M., and N. S. Chandel. 2014. ROS function in redox signaling and oxidative stress. *Curr. Biol.* 24: R453-R462.
15. Yang, C. S., D. M. Shin, K. H. Kim, Z. W. Lee, C. H. Lee, S. G. Park, Y. S. Bae, and E. K. Jo. 2009. NADPH oxidase 2 interaction with TLR2 is required for efficient innate immune responses to mycobacteria via cathelicidin expression. *J. Immunol.* 182: 3696-3705.
16. Yuk, J. M., D. M. Shin, C. S. Yang, K. H. Kim, S. J. An, J. Rho, J. K. Park, and E. K. Jo. 2009. Role of apoptosis-regulating signal kinase 1 in innate immune responses by *Mycobacterium bovis* bacillus Calmette-Guerin. *Immunol. Cell Biol.* 87: 100-107.
17. Shin, D. M., J. M. Yuk, H. M. Lee, S. H. Lee, J. W. Son, C. V. Harding, J. M. Kim, R. L. Modlin, and E. K. Jo. 2010. Mycobacterial lipoprotein activates autophagy via TLR2/1/CD14 and a functional vitamin D receptor signalling. *Cell Microbiol.* 12: 1648-1665.
18. Howard, S. T., E. Rhoades, J. Recht, X. Pang, A. Alsup, R. Kolter, C. R. Lyons, and T. F. Byrd. 2006. Spontaneous reversion of *Mycobacterium abscessus* from a smooth to a rough morphotype is associated with reduced expression of glycopeptidolipid and reacquisition of an invasive phenotype. *Microbiology* 152: 1581-1590.
19. Byrd, T. F., and C. R. Lyons. 1999. Preliminary characterization of a *Mycobacterium abscessus* mutant in human and murine models of infection. *Infect. Immun.* 67: 4700-4707.
20. Kim, T. S., Y. S. Kim, H. Yoo, Y. K. Park, and E. K. Jo. 2014. Mycobacterium massiliense induces inflammatory responses in macrophages through Toll-like receptor 2 and c-Jun N-terminal kinase. *J. Clin. Immunol.* 34: 212-223.
21. Kawai, T., and S. Akira. 2011. Toll-like receptors and their crosstalk with other innate receptors in infection and immunity. *Immunity* 34: 637-650.
22. Oeckinghaus, A., and S. Ghosh. 2009. The NF-kappaB family of transcription factors and its regulation. *Cold Spring Harb. Perspect. Biol.* 1: a000034.
23. Cruz-Knight, W., and L. Blake-Gumbs. 2013. Tuberculosis: an overview. *Prim. Care* 40: 743-756.
24. Huynh, K. K., S. A. Joshi, and E. J. Brown. 2011. A delicate dance: host response to mycobacteria. *Curr. Opin. Immunol.*

23: 464-472.

25. Marazzi, M. G., A. Chapgier, A. C. Defilippi, V. Pistoia, S. Mangini, C. Savioli, A. Dell'Acqua, J. Feinberg, E. Tortoli, and J. L. Casanova. 2010. Disseminated *Mycobacterium scrofulaceum* infection in a child with interferon-gamma receptor 1 deficiency. *Int. J. Infect. Dis.* 14: e167-e170.

26. Haas, W. H., P. Kirschner, S. Ziesing, H. J. Bremer, and E. C. Bottger. 1993. Cervical lymphadenitis in a child caused by a previously unknown mycobacterium. *J. Infect. Dis.* 167: 237-240.

27. Tortoli, E., P. Kirschner, B. Springer, A. Bartoloni, C. Burrini, A. Mantella, M. Scagnelli, C. Scarparo, M. T. Simonetti, and E. C. Bottger. 1997. Cervical lymphadenitis due to an unusual mycobacterium. *Eur. J. Clin. Microbiol. Infect. Dis.* 16: 308-311.

28. Kamala, T., C. N. Paramasivan, D. Herbert, P. Venkatesan, and R. Prabhakar. 1994. Isolation and Identification of Environmental Mycobacteria in the *Mycobacterium bovis* BCG Trial Area of South India. *Appl. Environ. Microbiol.* 60: 2180-2183.

29. Torvinen, E., S. Suomalainen, L. Paulin, and J. Kusnetsov. 2014. Mycobacteria in Finnish cooling tower waters. *APMIS* 122: 353-358.

30. Puthanakit, T., P. Oberdorfer, N. Ukarapol, N. Akarathum, S. Punjaisee, T. Sirisanthana, and V. Sirisanthana. 2006. Immune reconstitution syndrome from nontuberculous mycobacterial infection after initiation of antiretroviral therapy in children with HIV infection. *Pediatr. Infect. Dis. J.* 25: 645-648.

31. Brandt, L., C. J. Feino, O. A. Weinreich, B. Chilima, P. Hirsch, R. Appelberg, and P. Andersen. 2002. Failure of the *Mycobacterium bovis* BCG vaccine: some species of environmental mycobacteria block multiplication of BCG and induction of protective immunity to tuberculosis. *Infect. Immun.* 70: 672-678.

32. Flaherty, D. K., B. Vesosky, G. L. Beamer, P. Stromberg, and J. Turner. 2006. Exposure to *Mycobacterium avium* can modulate established immunity against *Mycobacterium tuberculosis* infection generated by *Mycobacterium bovis* BCG vaccination. *J. Leukoc. Biol.* 80: 1262-1271.

33. Barrow, W. W., and P. J. Brennan. 1982. Isolation in high frequency of rough variants of *Mycobacterium intracellulare* lacking C-mycoside glycopeptidolipid antigens. *J. Bacteriol.* 150: 381-384.

34. Recht, J., and R. Kolter. 2001. Glycopeptidolipid acetylation affects sliding motility and biofilm formation in *Mycobacterium smegmatis*. *J. Bacteriol.* 183: 5718-5724.

35. Bernut, A., J. L. Herrmann, K. Kissa, J. F. Dubremetz, J. L. Gaillard, G. Lutfalla, and L. Kremer. 2014. *Mycobacterium abscessus* cording prevents phagocytosis and promotes abscess formation. *Proc. Natl. Acad. Sci. U. S. A.* 111: E943-E952.

36. Rhoades, E. R., A. S. Archambault, R. Greendyke, F. F. Hsu, C. Streeter, and T. F. Byrd. 2009. *Mycobacterium abscessus* Glycopeptidolipids mask underlying cell wall phosphatidyl-myo-inositol mannosides blocking induction of human macrophage TNF-alpha by preventing interaction with TLR2. *J. Immunol.* 183: 1997-2007.

37. Jonsson, B., M. Ridell, and A. E. Wold. 2013. Phagocytosis and cytokine response to rough and smooth colony variants of *Mycobacterium abscessus* by human peripheral blood mononuclear cells. *APMIS* 121: 45-55.

38. Means, T. K., S. Wang, E. Lien, A. Yoshimura, D. T. Golenbock, and M. J. Fenton. 1999. Human toll-like receptors mediate cellular activation by *Mycobacterium tuberculosis*. *J. Immunol.* 163: 3920-3927.

39. Wang, T., W. P. Lafuse, and B. S. Zwilling. 2000. Regulation of toll-like receptor 2 expression by macrophages following *Mycobacterium avium* infection. *J. Immunol.* 165: 6308-6313.

40. Vignal, C., Y. Guerardel, L. Kremer, M. Masson, D. Legrand, J. Mazurier, and E. Elass. 2003. Lipomannans, but not lipoarabinomannans, purified from *Mycobacterium chelonae* and *Mycobacterium kansasii* induce TNF-alpha and IL-8 secretion by a CD14-toll-like receptor 2-dependent mechanism. *J. Immunol.* 171: 2014-2023.

41. Kleinnijenhuis, J., M. Oosting, L. A. Joosten, M. G. Netea, and C. R. Van. 2011. Innate immune recognition of *Mycobacterium tuberculosis*. *Clin. Dev. Immunol.* 2011: 405310.

42. Fremond, C. M., D. Togbe, E. Doz, S. Rose, V. Vasseur, I. Maillet, M. Jacobs, B. Ryffel, and V. F. Quesniaux. 2007. IL-1 receptor-mediated signal is an essential component of MyD88-dependent innate response to *Mycobacterium tuberculosis* infection. *J. Immunol.* 179: 1178-1189.

43. Yoshida, A., H. Inagawa, C. Kohchi, T. Nishizawa, and G. Soma. 2009. The role of toll-like receptor 2 in survival strategies of *Mycobacterium tuberculosis* in macrophage phagosomes. *Anticancer Res.* 29: 907-910.

44. Koul, A., T. Herget, B. Klebl, and A. Ullrich. 2004. Interplay between mycobacteria and host signalling pathways. *Nat. Rev. Microbiol.* 2: 189-202.

45. Schorey, J. S., and A. M. Cooper. 2003. Macrophage signalling upon mycobacterial infection: the MAP kinases lead the way. *Cell Microbiol.* 5: 133-142.

46. Jung, S. B., C. S. Yang, J. S. Lee, A. R. Shin, S. S. Jung, J. W. Son, C. V. Harding, H. J. Kim, J. K. Park, T. H. Paik, C. H. Song, and E. K. Jo. 2006. The mycobacterial 38-kilodalton glycolipoprotein antigen activates the mitogen-activated protein kinase pathway and release of proinflammatory cytokines through Toll-like receptors 2 and 4 in human monocytes. *Infect. Immun.* 74: 2686-2696.

47. Sim, Y. S., S. Y. Kim, E. J. Kim, S. J. Shin, and W. J. Koh. 2012. Impaired Expression of MAPK Is Associated with the Downregulation of TNF-alpha, IL-6, and IL-10 in *Mycobacterium abscessus* Lung Disease. *Tuberc. Respir. Dis. (Seoul.)* 72: 275-283.

48. Launois, P., M. Niang, A. Dieye, J. L. Sarthou, F. Rivier, and J. Millan. 1992. Human phagocyte respiratory burst by *Mycobacterium bovis* BCG and *M. leprae*: functional activation by BCG is mediated by complement and its receptors on monocytes. *Int. J. Lepr. Other Mycobact. Dis.* 60: 225-233.

49. Ferrari, C. K., P. C. Souto, E. L. Franca, and A. C. Honorio-Franca. 2011. Oxidative and nitrosative stress on phagocytes' function: from effective defense to immunity evasion mechanisms. *Arch. Immunol. Ther. Exp. (Warsz.)* 59: 441-448.

50. Vazquez-Torres, A. and F. C. Fang. 2001. Oxygen-dependent anti-Salmonella activity of macrophages. *Trends Microbiol.* 9:

29-33.

51. Lim, Y. J., H. H. Choi, J. A. Choi, J. A. Jeong, S. N. Cho, J. H. Lee, J. B. Park, H. J. Kim, and C. H. Song. 2013. *Mycobacterium kansasii*-induced death of murine macrophages involves endoplasmic reticulum stress responses mediated by reactive oxygen species generation or calpain activation. *Apoptosis* 18: 150-159.

52. Kim, J. J., H. M. Lee, D. M. Shin, W. Kim, J. M. Yuk, H. S. Jin, S. H. Lee, G. H. Cha, J. M. Kim, Z. W. Lee, S. J. Shin, H. Yoo, Y. K. Park, J. B. Park, J. Chung, T. Yoshimori, and E. K. Jo. 2012. Host cell autophagy activated by antibiotics is required for their effective antimycobacterial drug action. *Cell Host. Microbe* 11: 457-468.

53. Vilcheze, C., T. Hartman, B. Weinrick, and W. R. Jacobs, Jr. 2013. *Mycobacterium tuberculosis* is extraordinarily sensitive to killing by a vitamin C-induced Fenton reaction. *Nat. Commun.* 4: 1881.

54. Romero, M. M., L. Balboa, J. I. Basile, B. Lopez, V. Ritacco, S. S. de la Barrera, M. C. Sasiain, L. Barrera, and M. Aleman. 2012. Clinical isolates of *Mycobacterium tuberculosis* differ in their ability to induce respiratory burst and apoptosis in neutrophils as a possible mechanism of immune escape. *Clin. Dev. Immunol.* 2012: 152546.

55. Reddy, V. M., J. Luna-Herrera, and P. R. Gangadharam. 1996. Pathobiological significance of colony morphology in *Mycobacterium avium* complex. *Microb. Pathog.* 21: 97-109.

56. Sohn, H., H. J. Kim, J. M. Kim, K. O. Jung, W. J. Koh, and S. J. Shin. 2009. High virulent clinical isolates of *Mycobacterium abscessus* from patients with the upper lobe fibrocavitary form of pulmonary disease. *Microb. Pathog.* 47: 321-328.